ANALYSIS OF HUMAN TONE-BURST-EVOKED OTOACOUSTIC EMISSIONS

Reinhart Frosch
Sommerhaldenstrasse 5B, CH-5200 Brugg, Switzerland; reinifrosch@bluewin.ch
PSI (Paul Scherrer Institute), Villigen and ETH (Eidgenoessische Technische Hochschule), Zurich (retired)

1. INTRODUCTION

In one of my contributions to AWC-2010 in Victoria BC [Frosch (2010a)] it was shown that human click-evoked otoacoustic emissions (OAEs) documented in the literature agree with predictions based on cochlear maps. In a paper presented at the Forum Acusticum 2011 in Aalborg [Verhulst (2011)], human tone-burst-evoked OAEs appreciably different from those in Frosch (2010a) were shown. The purpose of the present study has been to find out if the OAEs in Verhulst (2011), too, agree with cochlear-map-based predictions.

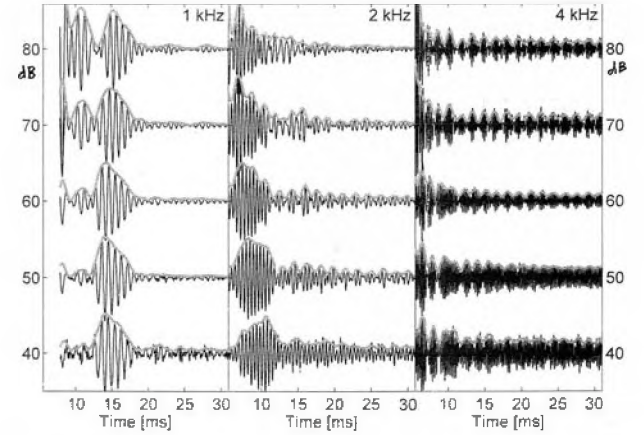

Figure 1. Waveforms of human tone-burst-evoked OAEs, reproduced with permission from Verhulst (2011).

The waveforms shown in Fig. 1 were generated by a tone burst emitted by an earphone inserted in an ear canal, and were recorded by a microphone; see Verhulst (2011) for details.

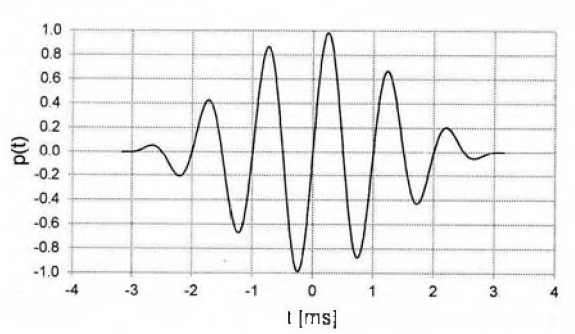

Figure 2. Sound-pressure function of the Hann-windowed tone burst used for the 1-kHz part of Fig. 1

The envelope of the tone burst in Fig. 2 is proportional to the squared cosine of ($\pi t/T$), where T = 6.3 ms.

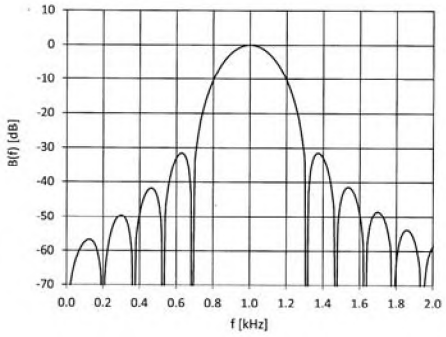

Figure 3. Spectral function of the tone-burst in Fig.2.

The corresponding spectral function, shown in Fig. 3, contains satellite peaks at –31dB, –41dB, etc.

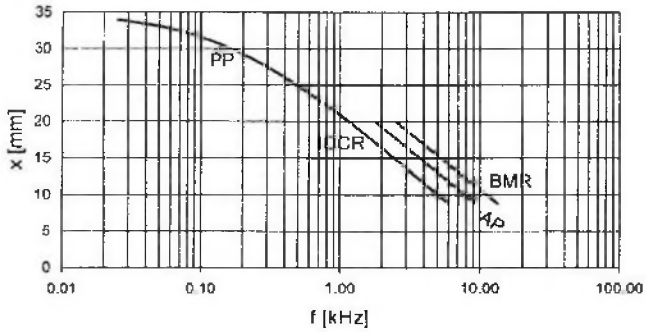

Figure 4. Human cochlear maps, reproduced from Fig. 3 of Frosch (2012).

In Fig. 4, four human cochlear maps are shown, namely the passive-peak (PP) map, the (low-level) active-peak (AP) map, the basilar-membrane resonator (BMR) map, and the internal organ-of-Corti resonator (IOCR) map. The IOCR map is hypothesized to coincide with the PP-map between 1 and 6 kHz, and is concluded to be not yet known at frequencies above and below that range. Cochlear maps are discussed in Chapters 33–41 of Frosch (2010b); a brief introduction is given in Frosch (2012).

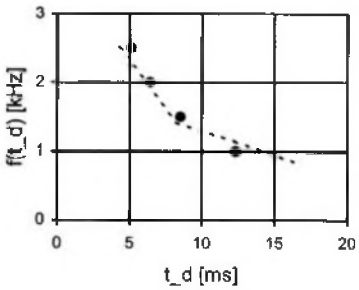

Fig. 5. Instantaneous click-evoked OAE frequency f versus OAE delay t_d; reproduced from Fig. 3 of Frosch (2010a).

The dashed line in Fig. 5 represents the instantaneous frequency of the human click-evoked OAEs according to Fig. 16.20 of Fastl and Zwicker (2007) [reproduced in Fig. 1 of Frosch (2010a)]. The filled circles in Fig. 5 represent the theoretical OAE delay $t_d(f) = 2\tau_{SW} + \tau_{rise}$; here, τ_{SW} is the surface-wave group travel time, from $x = 0$ to $x_{IOCR}(f)$ according to a box-model short-wave formula [Eq. (2) of Frosch (2010a)], and $\tau_{rise} = Q/(\pi \cdot f) \approx 1.3/f$ is the rise time of the forced oscillations of the internal organ-of-Corti resonators (IOCRs), which have a quality factor (resonance frequency divided by –3 dB resonance width) of $Q \approx 4$.

At $f = 1$ kHz, e.g., the IOCR-map place is $x_{IOCR} = 20.9$ mm (Fig.4), the just defined time durations are $\tau_{SW} = 5.5$ ms and $\tau_{rise} = 1.3$ ms, and the resulting OAE delay is $t_d = 12.3$ ms, as indicated in Fig. 5. A more detailed explanation of Fig. 5 is given in Chapter 44 of Frosch (2010b).

2. INTERPRETATION OF FIG. 1

1-kHz part, Time = 12-18 ms: OAEs transported by reverse travelling waves (TWs), emitted by OHCs in the 1-kHz IOCR resonance region (20 mm < x < 22 mm); center of primary tone burst is at Time = 3.15 ms; center of OAE burst is predicted to occur at Time = 3.15 ms + 12.3 ms = 15.45 ms, in agreement with Fig. 1.

1-kHz part, 80dB, Time = 7-14 ms: OAEs transported by reverse TWs, emitted by OHCs in the IOCR resonance regions of the high-frequency satellite peaks (1.37 kHz, 1.54 kHz, etc.; Fig. 3), superimposed on a decaying 1-kHz oscillation generated by the primary tone burst, but not due to an OAE. The satellite peaks of an 80-dB tone burst have sound-pressure levels (SPLs) of 49dB, 39dB, etc., and are therefore strongly amplified by the OHCs in their IOCR resonance regions. A part of the mechanical energy generated by these OHCs is transported back to the cochlear base by a reverse TW and thus causes OAEs.

1-kHz part, 80 dB, Time > 18 ms: Here, the OAEs due to the low-frequency satellite peaks (0.63 kHz, 0.46 kHz, etc.) are expected; they are negligibly weak, however, because the OHCs feed little mechanical energy into low-frequency TWs; see Chapter 35 of Frosch (2010b).

2-kHz part, 80 dB, Time = 11-15 ms: Now, low-frequency satellite peaks are at 1.40 kHz, 1.13 kHz, etc.; at these frequencies, the OHCs do feed significant mechanical energy into TWs. The corresponding low-frequency OAE at Time = 11-15 ms is clearly visible in Fig. 1.

1-, 2-, and 4 kHz parts, 60-80 dB: At large delays, these OAEs form stationary beats, different from the mentioned click-evoked OAEs in Fig. 1 of Frosch (2010a), where a stationary 3-kHz oscillation, attributed to spontaneous OAEs (SOAEs) triggered by the click, was observed. The large-delay beats in the 1-kHz part of Fig. 1 are consistent with being due to the superposition of two SOAEs of 1.4 and 1.6 kHz. As an alternative to Shera (2003), these SOAEs are conjectured to be due to OHCs feeding energy into localized basilar-membrane (BM) oscillations in the 1-kHz IOCR resonance region (20mm < x < 22mm). In that region, the without-liquid BMR resonance frequencies range from 1.7 to 2.4 kHz (Fig. 4). In a real (liquid-filled) cochlea, the just mentioned BM oscillations are thought to involve standing evanescent liquid-pressure waves. As discussed in Frosch (2011), the frequency of such a with-liquid BM oscillation is lower than that of the local without-liquid oscillation by typically 0.24 octave, i.e., by a factor of $2^{-0.24} = 0.85$. Thus in the present case the predicted SOAE frequencies range from 1.4 to 2.0 kHz, and so are consistent with the mentioned experimental SOAE frequencies of 1.4 and 1.6 kHz.

f_0 [kHz]	f_1 [kHz]	f_2 [kHz]
1.0	1.4	1.6
2.0	1.5	2.1
4.0	3.4	4.1

Table 1. SOAE frequencies f_1, f_2 consistent with the stationary beats at large delays in Fig. 1; f_0 is the central frequency of the primary tone burst.

The large-delay beats in the 2- and 4-kHz parts of Fig. 1 are consistent with being due to the superposition of two SOAEs as listed in Table 1. These frequencies f_1, f_2 are below the range expected for SOAEs caused by OHCs feeding energy into BM oscillations in the IOCR resonance regions of f_0; they agree, however, with predictions based on the IOCR resonance regions of the highest satellite-peak frequencies below f_0, which for $f_0 = 2$ or 4 kHz are so high that the generated TWs are strongly amplified by the involved OHCs.

3. CONCLUSION

The tone-burst-evoked OAEs in Fig. 1, in spite of differing appreciably from the click-evoked OAEs in Fig. 1 of Frosch (2010a), are found to be compatible with predictions based on the human cochlear maps represented in Fig. 4.

REFERENCES

Fastl, H., Zwicker, E. (2007). Psychoacoustics, Facts and Models. Springer, Berlin, p. 335.

Frosch, R. (2010a). Analysis of Human Oto-Acoustic Emissions. Canadian Acoustics, Vol. 38, No. 3, 88-89.

Frosch, R. (2010b). Introduction to Cochlear Waves. vdf, Zurich, pp. 331-386.

Frosch, R. (2011). Cochlear Evanescent Liquid Sound-Pressure Waves During Spontaneous Oto-Acoustic Emissions. Canadian Acoustics, Vol.39, No.3, 122-123.

Frosch, R. (2012). Human Cochlear Maps. Contribution to this conference.

Shera, C.A. (2003). Mammalian spontaneous otoacoustic emissions are amplitude-stabilized cochlear standing waves. J. Acoust. Soc. Am. 114, 244-262.

Verhulst, S. (2011). Investigating the Periodicity of Transient-Evoked Otoacoustic Emission Envelopes. Proceedings of Forum Acusticum 2011, Aalborg, pp. 1235-1240.